Int. J. Heat Mass Transfer. Vol. 30, No. 3, pp. 427–435, 1987
Printed in Great Britain

0017–9310/87 $3.00 + 0.00
Pergamon Journals Ltd.

Effect of yaw on forced convection heat transfer from a circular cylinder

E. M. SPARROW and A. A. YANEZ MORENO
Department of Mechanical Engineering, University of Minnesota, Minneapolis, MN 55455, U.S.A.

(*Received* 10 *April* 1986 *and in final form* 21 *July* 1986)

Abstract—Wind tunnel experiments encompassing ten angles of yaw between 0 (crossflow) and 60° yielded Nusselt numbers extending over the range of free stream Reynolds numbers from 9000 to 70,000. Supplementary experiments were also performed in which the heating pattern at the surface of the cylinder was varied and in which major alterations were made in the boundary layer on the wind tunnel wall. These experiments established that the measured Nusselt numbers were truly representative of the uniform wall temperature boundary condition and were independent of the characteristics of the wind tunnel boundary layer. It was found that as the cylinder was yawed relative to the crossflow orientation, the Nusselt number at first decreased, attained a minimum at a yaw angle of 15°, and then increased to a broad maximum which occurred in the range of yaw angles between 30 and 45°. Thereafter, the Nusselt number decreased with increasing yaw. Furthermore, the data did not obey the so-called Independence Principle, according to which the Nusselt number is supposed to be a unique function of the Reynolds number based on the component of the free stream velocity normal to the cylinder. As a further supplement to the heat transfer experiments, the pattern of fluid flow adjacent to the cylinder surface was visualized by means of the oil–lampblack technique.

INTRODUCTION

THIS PAPER is concerned with the response of the Nusselt number for a circular cylinder to the angle at which the cylinder is yawed relative to crossflow (i.e. crossflow corresponds to a yaw angle $\theta = 0°$). For cylinders other than wires, the relevant literature is represented by the heat transfer experiments of refs. [1, 2] and the mass transfer experiments of ref. [3]. At a given free stream Reynolds number, these studies yielded different variations of the Nusselt (Sherwood) number with the angle of yaw. In ref. [1], Nu decreased as the cylinder was yawed from crossflow to $\theta = 30°$, then increased slightly in the range 30–50°, and decreased thereafter. On the other hand, in ref. [2], there was a monotonic decrease of Nu with θ. In ref. [3], Sh actually increased slightly as the yaw ranged from $\theta = 0$ to 15° and subsequently decreased with further increases in yaw.

Despite the aforementioned non-monotonic behavior, it was concluded in refs. [1, 3] that the effect of yaw on the Nusselt number obeyed the so-called Independence Principle. According to that principle, the Nusselt number is supposed to be a unique function of the Reynolds number based on the velocity $U_\infty \cos\theta$, independent of the yaw angle. Such a representation implies a monotonic decrease of Nu with θ at a fixed free stream Reynolds number (i.e. based on U_∞).

The present experiments were performed in air and encompassed ten yaw angles in the range between $\theta = 0$ and 60° and 7–8 values of the free stream Reynolds number between 9000 and 70,000. This represents a much denser parameterization than in the past. In addition, supplementary experiments were carried out to investigate the response of the cylinder heat transfer to alterations of the upstream thermal and fluid flow conditions. The latter included variation of the thickness of the boundary layer on the wind tunnel walls and the introduction of massive disturbances into the boundary layer. The former involved the absence or presence of heating at portions of the cylinder surface away from the test section zone where the heat transfer coefficients were measured.

EXPERIMENTS

A schematic side view of one of the yawed cylinders, that for $\theta = 45°$, is shown in Fig. 1(a). As seen there, the cylinder was a composite structure consisting of a heated test section flanked at either end by a guard heater and by a diagonally-cut extension used to set the angle of yaw. The test and guard sections were common to all the investigated yaws, with a specific pair of extension pieces used for each angle. The cylinder had an outer diameter of 5.08 cm, and the axial lengths of the test section and of each guard heater were 13.335 and 7.328 cm, respectively. Situated between the test section and the guard heaters were 0.3175-cm-thick spacers. The lengths of the extension pieces for each angle were chosen so that the overall vertical height of the cylinder would be 29.21 cm (equal to the height of the wind tunnel).

The test section and the guard heaters were fabricated with thick walls (0.953 cm) and from high conductivity materials (copper and aluminum, respectively) to ensure temperature uniformity. Heat-

NOMENCLATURE

A	surface area of cylinder test section	Re_N	Reynolds number based on $U_\infty \cos\theta$
D	cylinder diameter	T_w	cylinder wall temperature
h	heat transfer coefficient, equation (1)	T_∞	free stream temperature
k	thermal conductivity	U_∞	corrected free stream velocity, equation (2).
Nu	Nusselt number, hD/k		
Nu_0	Nusselt number for crossflow		
Q	heat transfer rate at cylinder test section	Greek symbols	
Re	free stream Reynolds number, $U_\infty D/\nu$	θ	angle of yaw ($\theta = 0°$ for crossflow)
		ν	kinematic viscosity.

ing was accomplished with uniformly wound, separately controllable resistance-wire cores. The test section was equipped with 15 fine-gage, precalibrated thermocouples, while three thermocouples were installed in each guard heater at locations aligned with adjacent test section thermocouples. The thermocouple junctions were situated about 0.05 cm from the surface of the cylinder.

During each data run, the temperatures of the test section and guard heaters were matched, thereby eliminating extraneous conduction losses from the test section. To increase the sensitivity of the temperature matching procedure, the aforementioned spacers, made of Delrin plastic (an insulator), were placed between the test section and the guard heaters. The extension pieces (Fig. 1(a)) were also of Delrin. Radiation losses from the test section were reduced to a negligible level by polishing the surface to a mirror finish.

The temperature of the free stream airflow was measured by a pair of thermocouples situated to the side of the cylinder and at midheight. The free stream velocity measurement was accomplished with an impact probe and adjacent wall static tap, both situated 25 cm upstream of the cylinder and to the side.

The experiments were performed in a low-speed, low-turbulence ($\sim 0.5\%$) wind tunnel operated in the open-circuit mode and in suction. The tunnel cross section was a 29.2×61.0 cm rectangle (height $\times$ width), with an overall length of 2.4 m. With the utilized instrumentation, temperatures were measured to 1 μV and pressures to 10^{-3} Torr.

Owing to the yaw, there is an axial fluid flow along the cylinder from bottom to top. The axial flow experiences hydrodynamic and thermal boundary layer development as it moves along the cylinder. Because of this, there was concern that the test section heat transfer coefficients might be affected by the absence of heating at the lower extension piece. This concern led to supplementary experiments using the cylinder shown in Fig. 1(b).

For that cylinder, the Delrin extension pieces were replaced with aluminum extension pieces which were equipped with thermocouples and independently controlled heater cores. By this, the extension pieces served as additional guard heaters whose temperatures were matched with those of the original guard heaters. As seen in Fig. 1(b), the sensitivity of the matching procedure was heightened by the installation of Delrin spacers between the new and original guard heaters. The lower extension piece was

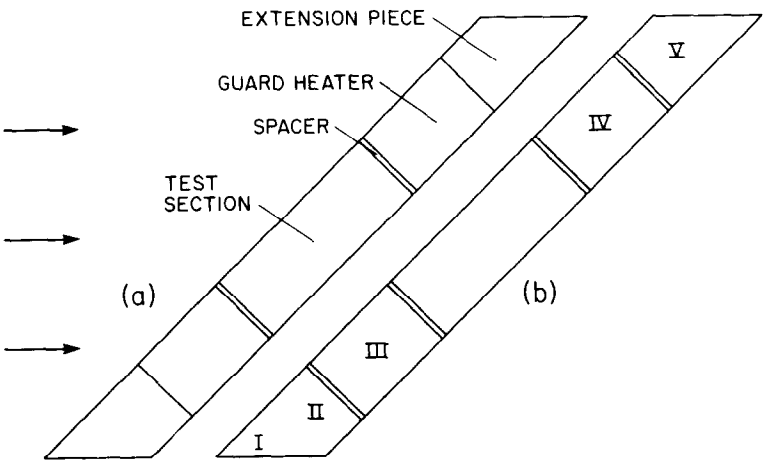

FIG. 1. Schematic side-view diagrams of representative yawed cylinders used in the experiments.

equipped with two independent heating circuits to provide finer temperature control upstream of the test section, with the result that there were five guard heaters, numbered I–V in Fig. 1(b).

Further information about the experimental apparatus and procedure is available in ref. [4].

In addition to the heat transfer experiments, flow visualization was performed using the oil–lampblack technique [5]. To facilitate these visualization experiments, the surface of the cylinder was covered with white, plastic-coated contact paper before the mixture of oil and lampblack powder was applied. When the airflow in the wind tunnel was initiated and maintained, the aerodynamic forces acting on the cylinder surface caused the mixture to move and take on a pattern indicative of the pattern of fluid flow adjacent to the cylinder. To obtain a record of the visualization pattern, the contact paper was removed from the cylinder surface, laid flat, and photographed.

DATA REDUCTION

The average heat transfer coefficient and Nusselt number for the test section portion of the cylinder were evaluated from their defining equations

$$h = Q/A(T_w - T_\infty), \quad Nu = hD/k. \tag{1}$$

The heat transfer rate appearing in the h equation was evaluated from the electric power input to the test section heater since the conduction losses were eliminated by the guard heating and the radiation losses were negligible ($\sim 0.2\%$ of Q). For the evaluation of the surface temperature T_w, the 15 test section thermocouples were averaged. The typical deviation of any thermocouple reading from the average was 0.2% of $(T_w - T_\infty)$. Similarly, the two free stream thermocouples were averaged to obtain T_∞, with typical percentage deviations being 0.1% of $(T_w - T_\infty)$. The quantities A and D in equation (1) denote the surface area of the test section and the cylinder diameter, respectively.

For the evaluation of the Reynolds number, account was taken of the fact that the presence of the cylinder results in an 8.3% blockage of the cross section of the wind tunnel. The blockage correction for the free stream velocity was based on equation (8a) of ref. [6] which, when evaluated for the condition of the experiments, yielded

$$U_\infty = 1.052\,(U_\infty)_{meas} \tag{2}$$

in which $(U_\infty)_{meas}$ is the free stream velocity measured upstream of the cylinder. Then, the free stream Reynolds number followed as

$$Re = U_\infty D/\nu. \tag{3}$$

A Reynolds number Re_N based on the component of the free stream velocity normal to the yawed cylinder is sometimes used as an alternative to the free stream Reynolds number, i.e.

$$Re_N = (U_\infty \cos\theta)D/\nu = Re\cos\theta. \tag{4}$$

The thermophysical properties appearing in equations (1), (2), and (4) were evaluated at a reference temperature $(T_w + T_\infty)/2$.

RESULTS AND DISCUSSION

Establishment of the results

The experiments performed to establish the generality of the results will now be described. The first set of experiments was carried out with the cylinder in crossflow. From the oil–lampblack flow visualizations, it was verified that the test section portion of the cylinder was far removed from direct interaction with the boundary layers on the wind tunnel walls. Therefore, the measured Nusselt numbers were free from end effects.

The crossflow Nusselt numbers are plotted in Fig. 2(a) as a function of the free stream Reynolds number Re. Also appearing in the figure is a curve representing the correlation of Churchill and Bernstein [7]. This correlation is the most recent of the numerous available correlations for heat transfer to a cylinder in crossflow and is, seemingly, the most encompassing. From the figure, it is seen that the deviations between the data and the correlation are in the 5% range. When viewed relative to the spread of the data on which crossflow Nusselt number correlations are based, the level of agreement in evidence in Fig. 1(a) is highly satisfactory. This agreement lends support to the proper functioning of the apparatus and proper execution of the experiments.

The next issue to be addressed is whether the test section heat transfer is affected by the absence or presence of heating at the outboard portions of the cylinder (i.e. at the extension pieces). As discussed earlier, the yaw gives rise to an axial flow along the cylinder from bottom to top, and it is this axial flow that may carry information about the outboard-piece heating to the test section.

Figure 2(b) conveys information that provides a firm conclusion about this issue. In the figure, the Nusselt–Reynolds variation for the case of 45° yaw is plotted for the two heating conditions represented by Figs. 1(a) and (b). The data for these cases are labeled *unheated extension pieces* and *completely heated cylinder*, respectively. Despite the expanded ordinate scale of the figure, the data for the two heating conditions are seen to be nearly coincident, with deviations confined to the 1–2% range. These deviations are, in fact, within the reproducibility of the data, which is about 2%. It may, therefore, be concluded that the present test section Nusselt numbers are universal with respect to the uniform wall temperature boundary condition.

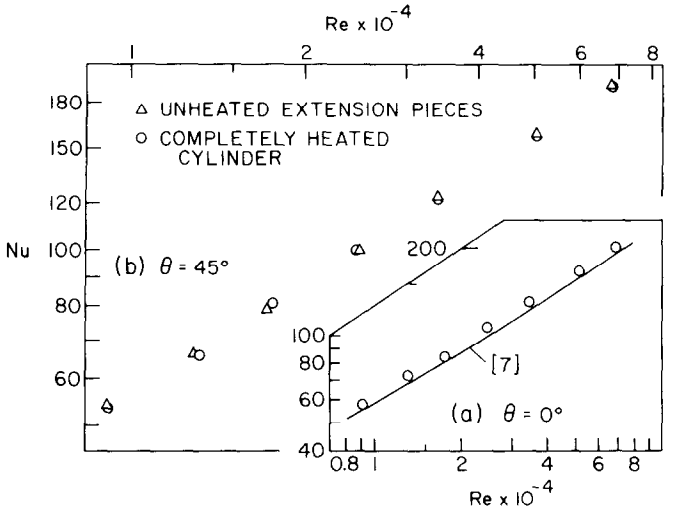

FIG. 2. Nusselt number comparisons for (a) crossflow and (b) 45° yaw.

The other experiments performed to establish the generality of the results were concerned with the hydrodynamics of the flow approaching the cylinder. These studies were carried out using the cylinder of Fig. 1(b), i.e. for a yaw angle $\theta = 45°$. In the first of these experiments, the forwardmost edge of the cylinder, which had been situated about 71 cm downstream of the inlet section of the tunnel test section, was moved forward to a position 50 cm from the inlet section. The motivation for this repositioning was to determine if the corresponding change in the boundary layer thickness at the forwardmost edge would affect the Nusselt number at the cylinder test section. For data runs performed over the same Reynolds number range as in Fig. 2(b), the Nusselt numbers measured for the repositioned cylinder were within $\pm 0.5\%$ of those at the original position.

Whereas the foregoing modification brought about a modest change in the approach-flow boundary layer as viewed by the cylinder, a traumatic change was imposed in subsequent experiments. This was accomplished by placing a solid bar of square cross section on the floor of the wind tunnel at a point 15 cm upstream of the forwardmost edge of the cylinder. Two bars were used (one at a time), with respective side-of-square dimensions of 0.635 and 1.27 cm. The bar-induced disturbances of the flow were greatest at the higher Reynolds numbers, so that the experiments were concentrated in that range.

Table 1 conveys the changes in the Nusselt number due to the perturbation bars. As expected, the presence of the perturbations increases the Nusselt number, with a greater effect at larger Re and for a larger bar. Of even greater importance is the fact that the change in Nu is remarkably small relative to the extent of the disturbance. From this it follows that the Nusselt number results are virtually independent of the characteristics of the wind tunnel boundary layer.

Table 1. Effect of perturbation bars on Nu

	Percent change in Nu	
Re	0.635 cm bar	1.27 cm bar
34,000	+ 0.69	+ 1.75
58,000	+ 2.66	+ 3.35

The experiments described in this section of the paper have demonstrated that the measured Nusselt numbers are universal with respect to the uniform wall temperature boundary condition and are independent of the characteristics of the wind tunnel boundary layer. With the generality of the results now established, attention will now be turned to the effect of yaw on the Nusselt number.

Response of Nu to yaw

The Nusselt numbers for each of the ten investigated angles of yaw are plotted as a function of the free stream Reynolds number in Fig. 3. To provide continuity, a least-squares straight line to the form

$$Nu = C\,Re^n \tag{5}$$

has been passed through the data for each yaw angle. The numerical values of C and n are listed in Table 2.

From an overview of the figure, it is seen that the results for the various yaw angles are not ordered in a regular manner. In particular, the data for the 0, 5, and 30° yaw angles fall closely together in the upper part of the band, below which there is a second cluster of data which encompasses $\theta = 10$, 25, and 45°. The lower group of data includes $\theta = 15$, 20, 55, and 60°, with a tendency for the curves for the various yaw angles to cross as Re increases.

Although the crossflow case ($\theta = 0°$) and the 5°, small-yaw case yield the highest Nu values, those for the $\theta = 30°$ yaw are virtually at the same level. On the other hand, the 15°-yaw Nusselt numbers are

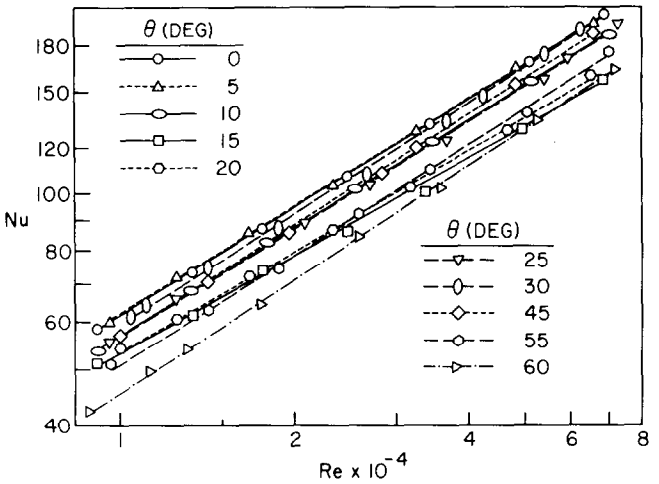

FIG. 3. Variation of the Nusselt number with the free stream Reynolds number for yaw angles between 0 and 60°.

Table 2. The constants C and n for equation (5)

θ (deg.)	C	n
0	0.207	0.618
5	0.217	0.614
10	0.200	0.614
15	0.302	0.561
20	0.270	0.574
25	0.187	0.620
30	0.172	0.634
45	0.161	0.636
55	0.152	0.630
60	0.113	0.651

quite low. Thus, it appears that the Nu vs θ variation is undulating, and this will be explored in more detail shortly.

Examination of Table 2 shows that the slope of the Nu–Re variation, as represented by the exponent n, is not very sensitive to the angle of yaw. For the most part, n is in the neighborhood of the crossflow value of 0.62. Somewhat lower values of n, 0.56–0.57, occur for $\theta = 15$ and 20°. It will be seen later that these θ values correspond to a trough in the Nu vs θ distributions.

The prominence of the Independence Principle suggests that the data be replotted as Nu vs Re_N, where Re_N is based on the component of the free stream velocity normal to the cylinder. Such a graph, prepared by employing equation (5), is presented in Fig. 4. Each curve is identified by a single symbol (not an actual data point) positioned so as not to conflict with adjacent curves. The symbols are the same as those of Fig. 3.

Inspection of the figure shows that the use of Re_N has not brought together the data for the various yaw angles. Indeed, the spread of the data in the Nu–Re_N format is greater than that in the Nu–Re format. Thus, the Independence Principle does not apply for the present results. Closer examination of the figure reveals that the results for $\theta = 45$, 55, and 60° do fall together, but this is a limited portion of the overall range of interest. The most positive feature of the use of Re_N is that the $\theta = 0°$ case now falls in the middle of the data band.

As noted earlier, other heat/mass transfer investigators have encountered departures from the Independence Principle. Fluid flow information supporting such departures is provided by the experiments of ref. [8].

The variation of the Nusselt number with the angle of yaw will now be quantified, and Fig. 5 has been prepared for this purpose. This figure is a crossplot of Fig. 3, and the plotted symbols represent crossplot points rather than actual data. Figure 5(a) conveys the Nu vs θ distributions, while Fig. 5(b) presents normalized Nu/Nu_0 distributions, where Nu_0 is the crossflow Nusselt number.

Turning first to Fig. 5(a), it is seen that the effect of yaw is qualitatively similar for all of the investigated Reynolds numbers. The Nusselt number is unaffected by yaw in the range from 0 to 5° but then decreases and attains a minimum at $\theta = 15°$. With further increases in yaw, the Nusselt number increases and achieves a broad maximum in the range between $\theta = 30$ and 45°. The Nu value at the maximum is approximately equal to that for crossflow. Beyond $\theta = 45°$, there is a monotonic decrease of the Nusselt number.

The Nu/Nu_0 format of Fig. 5(b) provides a vehicle for appraising the magnitude of the undulations of Nu with θ. From the figure, it is seen that the minimum at $\theta = 15°$ is accentuated at higher Reynolds numbers, as witnessed by the fact that $Nu/Nu_0 = 0.87$ for $Re = 9000$ and 0.77 for $Re = 70{,}000$. At larger angles of yaw, this trend is reversed and the larger departures of Nu/Nu_0 from unity occur at smaller Re.

The complex variation of Nu with θ as documented by Fig. 5 is undoubtedly a reflection of changes in

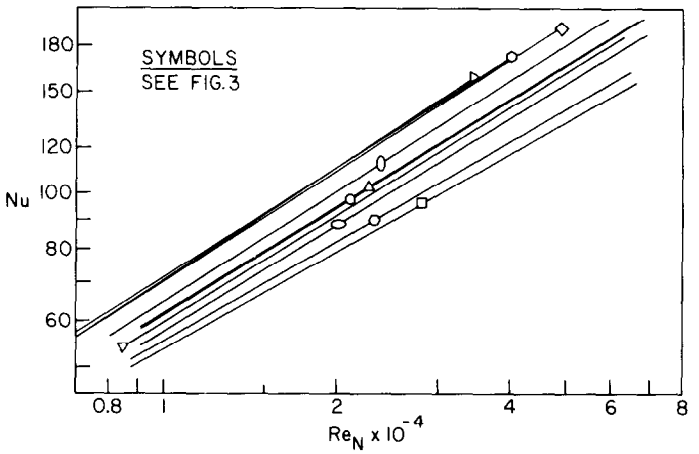

FIG. 4. Variation of the Nusselt number with the normal-component-based Reynolds number for yaw angles between 0 and 60°.

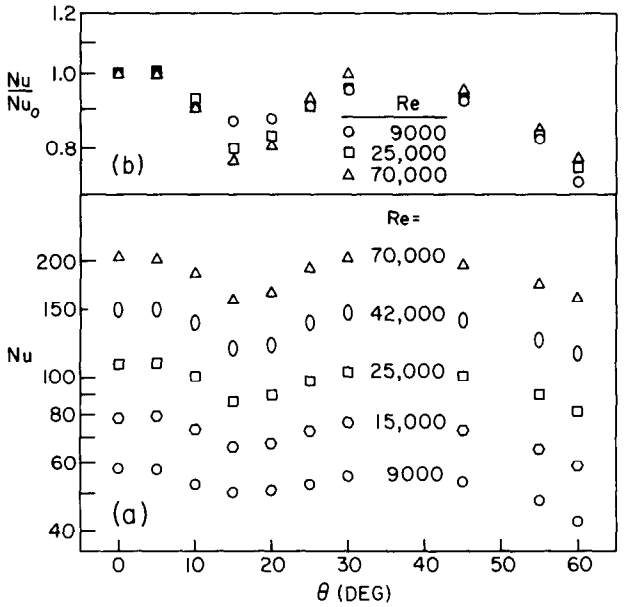

FIG. 5. Variation of the Nusselt number with the yaw angle for Reynolds numbers between 9000 and 70,000.

the pattern of fluid flow with yaw. An indication of these changes is provided by the flow visualization patterns that will now be presented.

Flow visualization patterns

Photographs of the oil–lampblack flow visualization patterns for $\theta = 15$ and 30° are presented in Figs. 6 and 7. They were selected from a larger collection in ref. [4] because they are the sharpest and clearest among those available and because they display noteworthy differences in the pattern of fluid flow.

What is shown in Figs. 6 and 7 are photographs of the contact paper that had covered the cylinder during a visualization run and that had been removed and laid flat immediately after the run was completed. The photographs were taken with the camera positioned perpendicular to the laid-out contact paper. Since the contact paper covered both the forward-thrusting lower end of the cylinder and the rear-thrusting upper end, its laid-out shape is not a rectangle, as can be seen in the figures. The view presented in the figures is that of an observer who is situated upstream of the cylinder and is looking downstream.

The main features of the visualization patterns are the central, black vertical line, the array of fine streaklines which emanate from the black line, and

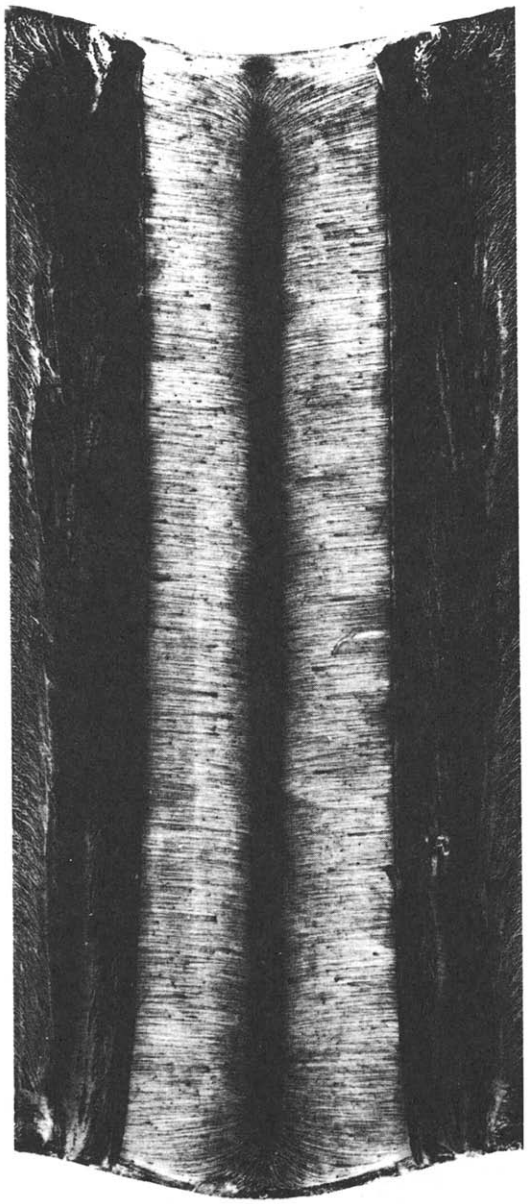

FIG. 6. Flow visualization pattern for 15° yaw.

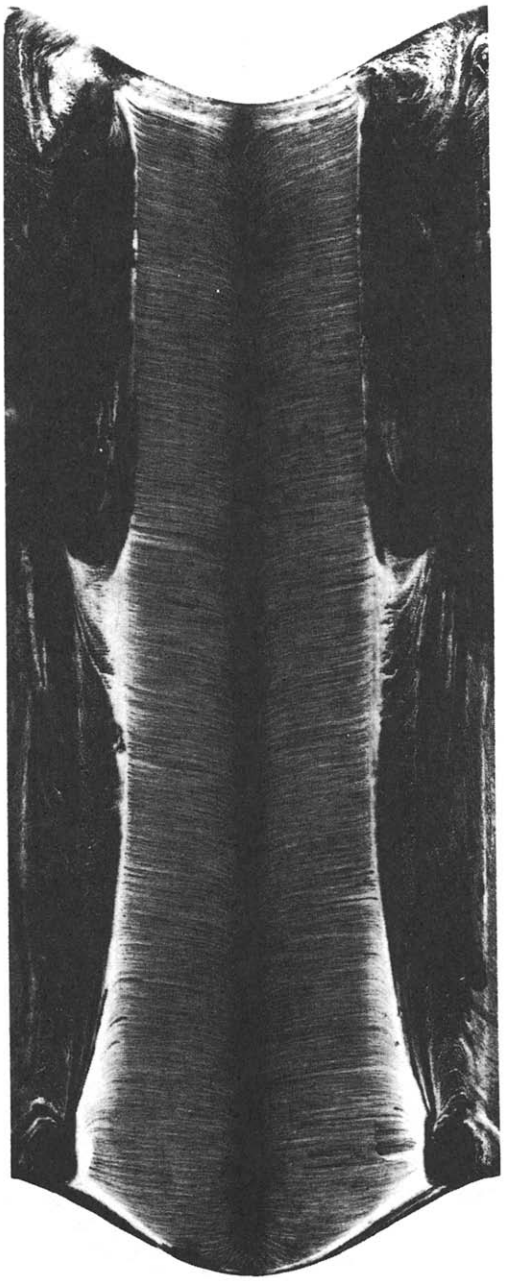

FIG. 7. Flow visualization pattern for 30° yaw.

the broad black bands which flank the streakline region. Respectively, these features correspond to the forward stagnation line, the boundary layer region on the forward portion of the cylinder, and the separated region on the rear portion of the cylinder. Part of the separated region has been masked off because it was marred by finger marks imprinted during the removal of the contact paper from the cylinder.

The fraying at the upper and lower ends of the stagnation line reflects the end effects due to the wind tunnel walls. Clearly, these end effects were far removed from the test section portion of the cylinder. The orientation of the streaklines relative to the stagnation line is markedly affected by the angle of yaw. For the crossflow case ($\theta = 0°$), the streaklines are perpendicular to the stagnation line. At the $\theta = 15°$ yaw (Fig. 6), the angle at which the streaklines emanate from the stagnation line deviates slightly from the perpendicular. This deviation indicates the presence of a yaw-related axial velocity component. As the fluid moves around the cylinder, there is a tendency for the direction of the streaklines to approach the perpendicular direction.

For the 30° yaw (Fig. 7), the streaklines emanating from the stagnation line emerge at an angle consider-

ably different than perpendicular, reflecting the presence of a strong axial velocity component. However, away from the stagnation line, the streaklines are oriented closer to the perpendicular direction, thereby indicating a lesser axial velocity component.

Aside from the aforementioned differences in the orientations of the streaklines (reflecting the different magnitudes of the axial velocity component), there are other noteworthy differences between the two flow patterns. The most dramatic of these is the intrusion of the boundary layer region into the separated region just above the midheight of the cylinder for the $\theta = 30°$ case. For the 15° case, no such intrusion was evident. The intrusion is believed responsible, at least in part, for the higher 30°-yaw Nusselt numbers. Another factor which may contribute to the higher 30° Nusselt numbers is the presence of strong vortices which flank each side of the boundary layer region adjacent to the top and bottom of the cylinder. These vortices are most clearly seen in Fig. 7 as black circles at the bottom of the cylinder, but they are also present at the top. The vortices are not in evidence in Fig. 6.

The aforementioned cause and effect relationships between specific fluid flow features and the response of the Nusselt number are necessarily conjectural. This is, however, the best that can be done with the available information.

CONCLUDING REMARKS

The experiments performed here have shown that the Nusselt number for a circular cylinder does not decrease monotonically as the cylinder is increasingly yawed relative to the crossflow orientation. Furthermore, the data do not obey the so-called Independence Principle, whereby the Nusselt number is supposed to be a unique function of the Reynolds number Re_N based on the component of the free stream velocity normal to the cylinder. As was discussed in the paper, other investigators have encountered non-monotonic variations of the Nusselt number with yaw angle, but in no case have the variations had the same form.

The present experiments were more densely parameterized with respect to yaw angle and Reynolds number than those of the past. Furthermore, a special feature of the present work was the supplementary experiments that were performed to establish the generality of the results. By altering the pattern of heating at the surface of the cylinder (either heating or not heating the outboard portions of the cylinder), it was established that the present results were universal with respect to the uniform wall temperature boundary condition. Furthermore, by drastically changing the nature of the boundary layer on the wind tunnel wall, it was demonstrated that the results were virtually independent of the characteristics of the wind tunnel boundary layer.

It is believed that the present Nusselt number results are the most generally characterized among those that are available for the yawed cylinder. Perhaps the only parameter remaining to be explored is the effect of free stream turbulence. The r.m.s. turbulence level in the present experiments was about 0.5%, which is typically regarded as low turbulence. However, this issue is still open since the response of the Nusselt number to free stream turbulence in the presence of yaw has not yet been established.

REFERENCES

1. J. S. Kraabel, A. A. McKillop and J. W. Baughn, Heat transfer to air from a yawed cylinder, *Int. J. Heat Mass Transfer* **25**, 409–418 (1982).
2. F. P. Kazakevitch, Effect of the angle of incidence of a gas stream on the heat transfer from a circular cylinder, *Zh. Tekh. Fiz.* **24**, 1341–1347 (1954).
3. R. E. Williams and R. G. Griskey, Mass transfer from cylinders at various orientations to flowing gas streams, *Can. J. Chem. Engng* **53**, 500–504 (1975).
4. A. A. Yanez Moreno, Heat transfer and pressure drop in a tube bank inclined with respect to the flow, Ph.D. thesis, Department of Mechanical Engineering, University of Minnesota, Minneapolis, Minnesota (1985).
5. W. Merzkirch, *Flow Visualization*. Academic Press, New York (1974).
6. V. T. Morgan, The overall convective heat transfer from smooth circular cylinders, *Adv. Heat Transfer* **11**, 199–264 (1975).
7. S. W. Churchill and M. Bernstein, A correlating equation for forced convection from gases and liquids to a circular cylinder in crossflow, *J. Heat Transfer* **99**, 300–306 (1977).
8. R. A. Smith, W. T. Moon and T. W. Kao, Experiments on flow about a yawed circular cylinder, *J. Basic Engng* **94**, 771–777 (1972).

EFFET DU DERAPAGE SUR LA CONVECTION THERMIQUE FORCEE AUTOUR D'UN CYLINDRE CIRCULAIRE

Résumé—Des essais en soufflerie avec des angles de dérapage entre 0 (écoulement frontal) et 60 fournissent des nombres de Nusselt pour des nombres de Reynolds entre 9000 et 70000. Des expériences supplémentaires sont effectuées pour des configurations de chauffage à la surface du cylindre variées et avec des altérations faites dans la couche limite sur les parois de la soufflerie. Ces expériences montrent que les nombres de Nusselt mesurés sont représentatifs de la condition limite de température de paroi uniforme et sont indépendants des caractéristiques de la couche limite de la soufflerie. On trouve que lorsque l'angle de dérapage par rapport à l'écoulement frontal augmente, le nombre de Nusselt décroît d'abord, atteint un minimum pour un angle de 15 et ensuite augmente jusqu'a un maximum qui se situe entre 30 et 45 . Au delà, le nombre de Nusselt décroît. Par suite, les données n'obéissent pas au Principe d'Indépendance selon lequel le nombre de Nusselt est supposé être une fonction unique du nombre de Reynolds basé sur la composante de vitesse incidenté normale au cylindre. En complément aux expériences de thermique, on visualise au moyen de fumée la structure de l'écoulement adjacent à la surface du cylindre.

DER EINFLUSS DES NEIGUNGSWINKELS AUF DEN WÄRMEÜBERGANG BEI ERZWUNGENER KONVEKTION AN EINEM KREISZYLINDER

Zusammenfassung—Im Rahmen von Windkanalexperimenten wurden Nusselt-Zahlen für in Strömungsrichtung zwischen 0° (Kreuzstrom) und 60° geneigte Kreiszylinder für Reynolds-Zahlen zwischen 9000 und 70 000 ermittelt. Ergänzende Experimente, bei denen die Heizleistung an der Zylinderoberfläche variiert und hauptsächlich die Grenzschicht an den Kanalwänden verändert wurde, wurden ebenfalls durchgeführt. Durch diese Experimente konnte nachgewiesen werden, daß die gemessenen Nusselt-Zahlen nur von der Randbedingung 1. Art abhängen und unabhängig von den Eigenschaften der Kanalgrenzschicht sind. Wie gezeigt werden konnte, nimmt die Nusselt-Zahl bei Zylinderdrehungen relativ zur Strömungsrichtung zuerst ab, erreicht bei einem Winkel von 15° ein Minimum und nimmt dann bis zum Erreichen eines absoluten Maximums bei einem Winkel von ungefähr 30 bis 45° wieder zu. Nach Überschreiten des Maximums nimmt die Nusselt-Zahl mit zunehmenden Drehwinkeln ab. Darüber hinaus konnte das sogenannte Unabhängigkeitsprinzip nicht bestätigt werden, wonach die Nusselt-Zahl als eindeutige Funktion der Reynolds-Zahl, die mit der Normalkomponente der Strömungsgeschwindigkeit senkrecht zur Zylinderoberfläche gebildet wird, dargestellt werden kann. Ergänzend zu den Wärmeübergangsexperimenten wurden Strömungsbilder nahe der Zylinderoberfläche mit Hilfe der Flamm–Ruß-Methode sichtbar gemacht.

ВЛИЯНИЕ УГЛА НАТЕКАНИЯ ПОТОКА НА ВЫНУЖДЕННО-КОНВЕКТИВНЫЙ ТЕПЛОПЕРЕНОС ОТ КРУГЛОГО ЦИЛИНДРА

Аннотация—В экспериментах, проведенных в аэродинамической трубе при десяти углах натекания потока в диапазоне от 0 (поперечное обтекание) до 60°, получены зависимости чисел Нуссельта от чисел Рейнольдса свободного потока в диапазоне от 9000 до 70000. В дополнительных экспериментах варьировался режим нагрева поверхности цилиндра, причем основные изменения наблюдались в пограничном слое на стенке аэродинамической трубы. Установлено, что измеренные значения чисел Нуссельта определяются граничными условиями с однородной температурой на стенке и не зависят от характеристик пограничного слоя аэродинамической трубы. Найдено, что при изменении наклона цилиндра число Нуссельта вначале убывает, достигая минимума при угле наклона 15°, а затем возрастает, и в диапазоне от 30° до 45° является максимальным. Далее, с увеличением угла наклона число Нуссельта уменьшается. Более того, результаты не подчиняются так называемому принципу независимости, из которого следует, что число Нуссельта является однозначной функцией числа Рейнольдса, построенной по компоненте скорости свободного потока, перпендикулярной цилиндру. Как дополнение к экспериментам по теплообмену, с помощью методики закопченого стекла визуализировался режим, течения жидкости, примыкающей к поверхности цилиндра.